Control of a Multiunit Heterogeneous Azeotropic Distillation Process

William L. Luyben
Process Modeling and Control Center, Dept. of Chemical Engineering, Lehigh University, Bethlehem, PA 18015

DOI 10.1002/aic.10650

An investigation of the design and control of a system in which a heterogeneous azeotrope permits the use of a decanter to cross a distillation boundary is reported. The specific numerical example is the classical production of anhydrous ethanol from an ethanol/water mixture using benzene as the entrainer. The feed is an ethanol/water mixture with composition that is near the binary azeotrope, which has been produced in an upstream binary distillation column. The process consists of two columns in which the addition of benzene takes the water out the top of the first column, producing high-purity ethanol out the bottom. The overhead vapor is condensed and forms two liquid phases. The organic benzene-rich phase provides reflux to the first column. The aqueous phase is fed to a second distillation column that produces high-purity water out the bottom and recycles the distillate back to the first column. The steady-state convergence of this two-column system with two-recycles if very difficult. Convergence is achieved by using a dynamic model. A plantwide control scheme is developed and is shown to provide stable base-level regulatory control for very large disturbances. The control structure has a counter-intuitive feature. The aqueous level in the decanter is controlled by manipulating the flow rate of the aqueous stream from the decanter. The action of the level controller is the reverse of what is used conventionally, that is, if the level is increasing, the exit flow rate is decreased*!* © 2005 American Institute of Chemical Engineers *AIChE J,* 52: 623–637, 2006
Keywords: azeotropic distillation, process control

Introduction

The design of azeotropic distillation systems has been the subject of innumerable textbooks and papers for most of the last century. The 1922 pioneering book of Robinson and Gilliland[1] used trial-and-error manual tray-to-tray methods. The recent books by Doherty and Malone[2] and by Stichlmair and Fair[3] provide much more extensive analyses of these types of systems. The use of ternary-phase diagrams with distillation boundaries and residue curves is presented in these books, which provide very useful insight into the constraints encountered in these highly nonideal liquid–liquid–vapor systems. Current commercial process simulators (Aspen Split and DISTIL) facilitate the analysis of these systems.

The presence of an azeotrope in a binary system presents a limit (a distillation boundary) for the product compositions achievable in a single distillation column. For example, the ethanol/water system at atmospheric pressure has a homogeneous azeotrope at 351 K of composition 90 mol % ethanol. A typical mixture from a fermentation process has very low ethanol concentrations (4–6 mol %). If this mixture is fed to a distillation column operating at atmospheric pressure, high-purity water can be produced out from the bottom but the ethanol purity of the distillate cannot exceed 90 mol %.

Sometimes binary azeotropic mixtures can be separated by using two columns that operate at different pressures. This flowsheet is effective if the composition of the azeotrope shifts significantly with pressure. This method has the important advantage of not introducing other components, which can

---

Correspondence concerning this article should be addressed to W. L. Luyben at WLL0@Lehigh.edu.

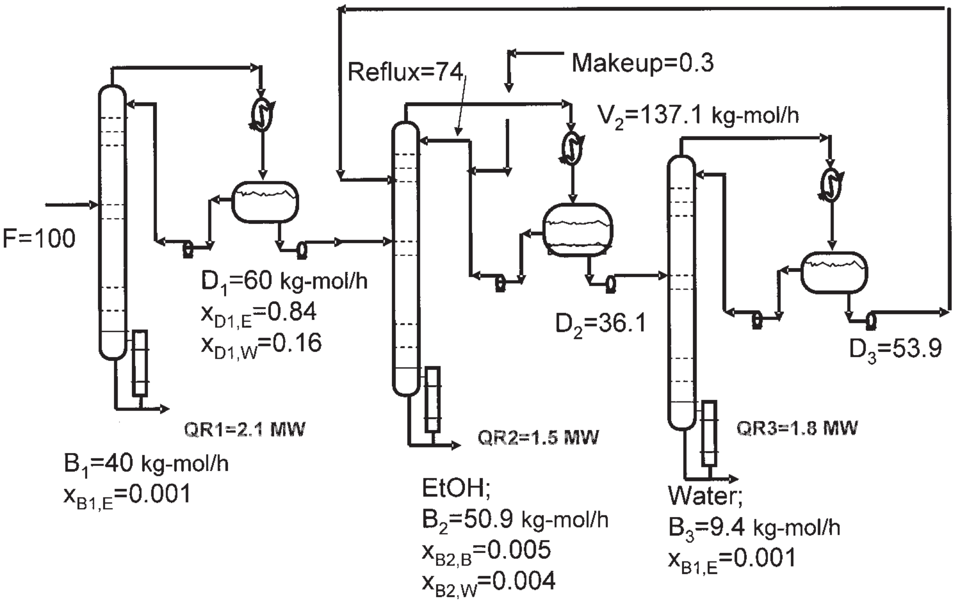

Figure 1. Flowsheet of three-column process.

present problems because of small traces of impurities in the final products.

Another common method to overcome binary azeotropes is to add a third component that produces a favorable impact on the relative volatilities of the two primary components. If the third component is less volatile and preferentially attracts one of the components, it can be used as a "solvent" in a two-column "extractive distillation" flowsheet. In the first column, the solvent is added near the top of the column. The nonattracted component goes overhead, and the solvent and attracted component go out the bottom. This stream is fed to a second distillation column that removes the attracted component overhead and recycles fresh solvent back to the first column.

If the third component is a "light entrainer" and goes overhead in the first column while preferentially taking one of the primary components with it and if this overhead forms two liquid phases, a two-column heterogeneous azeotropic flowsheet can be used. The light "organic" phase is refluxed back to the first column. The heavy "aqueous" phase is fed to the second column that produces high-purity product out the bottom and a distillate stream, that is recycled back to the first column. Figure 1 illustrates this flowsheet.

This type of system is the subject of this communication. The ethanol/water separation, studied in detail by Ryan and Doherty,[4] is used as a numerical example. The difficulties of performing the steady-state design of this highly nonlinear system with two recycle streams are discussed. Then a control scheme is developed that effectively handles very large disturbances to the system.

A similar system has been studied by Chien and coworkers.[5-8] They studied the heterogeneous azeotropic system of isopropyl alcohol, cyclohexane, and water. Both design and control issues were presented, as well as experimental results. In the first three papers, the azeotropic column was considered in isolation. In the last paper, a two-column system was explored. The control structure they developed for the two-column system uses an "inverse double-loop" strategy in the azeotropic column in which multiple temperatures are used. Their control structure is significantly different from the one developed in this article. It does not contain any counter-intuitive loops. In this report the control of only one temperature in each column is shown to provide good product quality control.

Process Studied

Figure 1 shows the flowsheet with steady-state design values for flow rates and compositions. Design parameters are based on those suggested by Ryan and Doherty[4] with some modifications. The feed stream enters the "preconcentrator column" C1. The distillate from this column D_1 is fed to the second "azeotropic column" C2 at a rate of 60 kmol h^{-1} (84 mol % ethanol and 16 mol % water). Column C2 has no condenser and 31 stages (Aspen notation: Stage 1 is the top tray and Stage 31 is the partial reboiler). The column operates at 2 atm and has three feed streams. Fresh feed enters on Stage 15, recycle from the second column enters on Stage 10, and the organic phase from the decanter is refluxed to the top tray. In addition, a very small make-up stream of benzene is added to account for the small losses. The bottoms product B_2 from C2 is high-purity ethanol. The reboiler heat input in C2 is 1.52 MW.

Overhead vapor from C2 is condensed, and the two liquid phases are separated in a decanter. The organic phase returns to C2. The aqueous phase D_2 (sometimes referred to in later sections as "F3") is fed to Stage 11 of the second column C3, the "entrainer recovery" column, which has 21 stages and operates at 1.1 atm. The distillate D_3 is recycled back to C2. The bottoms B_3 is high-purity water. The reflux ratio in C3 is 2. The reboiler heat input in C3 is 1.80 MW.

The commercial process simulator Aspen Plus is used for the steady-state design and AspenDynamics for the dynamic simulation. The UNIQUAC physical property package is used for the liquid–liquid–vapor phase equilibrium calculations.

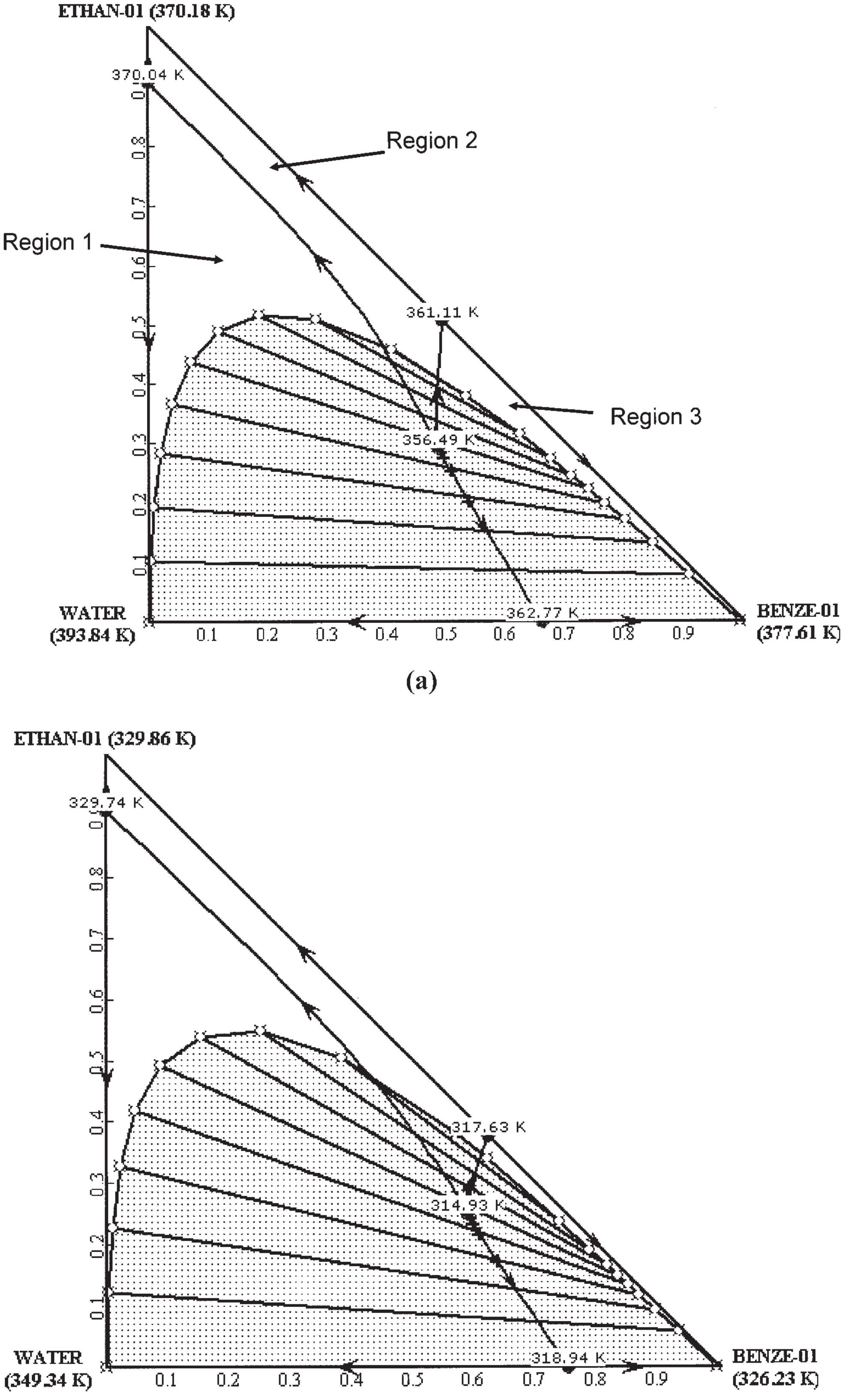

Figure 2. Benzene/ethanol/water at (A) 2 atm and (B) 0.4 atm.

Phase Equilibrium and Ternary Diagrams

The discussion in this section follows the standard analysis methods discussed in many textbooks and is presented to provide some understanding of the important concepts and aspects of these types of systems. The complexity of the phase equilibrium is displayed in the ternary diagrams shown in Figure 2. Figure 2A is with a pressure of 2 atm, the operating pressure in C2. Figure 2B is with a pressure of 0.4 atm, where the temperature of the ternary heterogeneous azeotrope is 315 K. This second diagram is shown because the temperature in the decanter is set at 315 K, not the 356 K that corresponds to a pressure of 2 atm. The column operates at 2 atm, which is held by a control valve in the overhead vapor line. The pressure downstream of the valve is atmospheric, but the condenser subcools the liquid to 315 K (as low a temperature as possible with cooling water to improve liquid–liquid phase separation). The decanter liquid phases are subcooled, with inert gas (air) maintaining the total pressure of 1 atm.

These ternary diagrams show the existence of two binary homogeneous azeotropes, one binary heterogeneous azeotrope, and one ternary heterogeneous azeotrope. The distillation boundaries separate the composition space into three regions. The desired ethanol product is in Region 2 near the pure ethanol apex of the triangular diagram. The desired water product is in Region 1 near the lower left corner. Because a distillation boundary separates these two products, the desired separation cannot be achieved in a single column.

As explained in detail in several references, it is insightful to locate the various streams on the ternary diagram. Figure 3A shows the entire three-column flowsheet and isolates the first column. A feed composition of 60 mol % ethanol is used for purposes of illustration. The stream fed to column C1 is *F*, and the streams leaving are B_1 and D_1. Figure 3B shows the locations of these streams on the ternary diagram. Because of the ternary mixing rule, the three points must lie on a straight line, which is along the ordinate in Figure 3B. The distillate is near the azeotrope.

Next let us consider column C3 because it is also a simple single-feed, two-product column. Figure 4A shows that its feed is the aqueous stream D_2 from the decanter with composition $x_{Aqueous}$. The product streams are D_3 and B_3. The latter is high-purity water. As shown in Figure 4B, these three points lie on a straight line in Region 1.

Now let us turn to the more difficult analysis of column C2. We will consider it in two ways: first, with the decanter included and second without the decanter. Figure 5A shows the flowsheet with C2 and the decanter considered. The inputs to this system are D_1 and D_3. The outputs are B_2 and D_2. If we graphically "mix" the two inputs into a pseudo stream M, as shown in Figure 5B, the B_2 and D_2 points must lie on a straight line that goes through the M point.

It is important to note that the two products from this column/decanter coupled system lie in *different* regions of the diagram. The existence of the decanter permits the distillation boundary to be crossed.

Finally let us consider the column C2 in isolation without the decanter as shown in Figure 6A. This system has three inputs: D_1, D_3, and the organic reflux; and it has two outputs: V_2 and B_2. If we graphically "mix" the three inputs into a pseudo stream M2, the V_2 and B_2 points must lie on a straight line that goes through the M2 point, as shown in Figure 6B. The ternary diagram is generated for a pressure of 0.4 atm because this corresponds to a decanter temperature of 315 K, which was used in the rigorous simulation design study discussed in the next section.

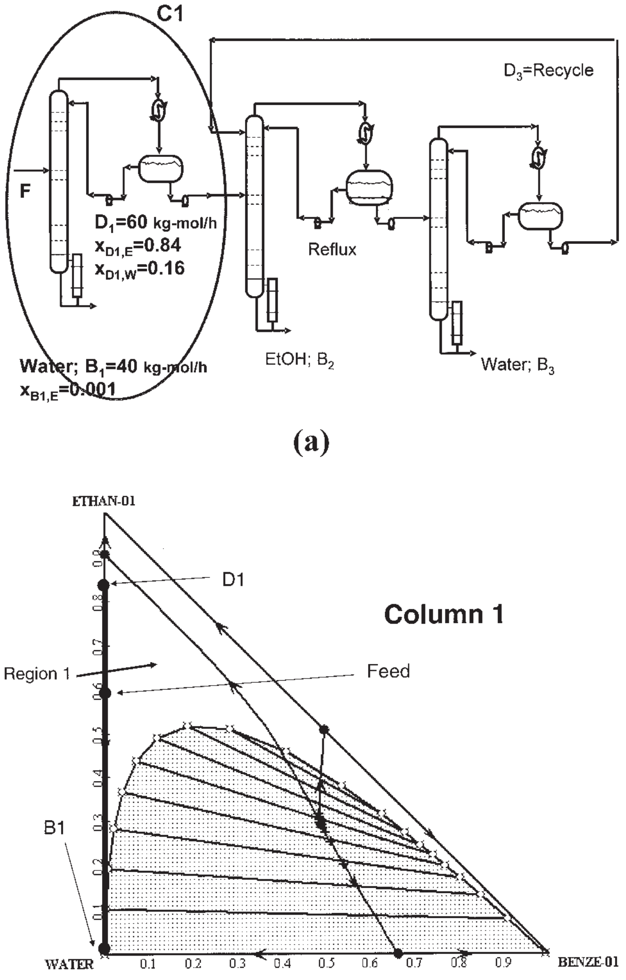

(a)

(b)

Figure 3. (A) Column C1; (B) location of streams in column C1.

Note that the V_2 and B_2 points both lie in Region 2, and no distillation boundaries are crossed.

The organic phase has a composition $x_{Organic}$, which lies at the benzene-rich side of the liquid–liquid equilibrium envelop. The organic and aqueous phases lie at opposite ends of the liquid–liquid equilibrium tie-line shown in Figure 6B. The vapor V_2 from column C2 lies somewhere along the same tie-line. Steady-state conditions and design parameter values are summarized in Tables 1 and 2. Figure 7 shows the three-column flowsheet with steady-state conditions.

Steady-State Design

The results given in the previous section and summarized in Tables 1 and 2 were obtained from a rigorous simulation of the process, but not without a significant expenditure of time and effort. Aspen Plus was used to develop the steady-

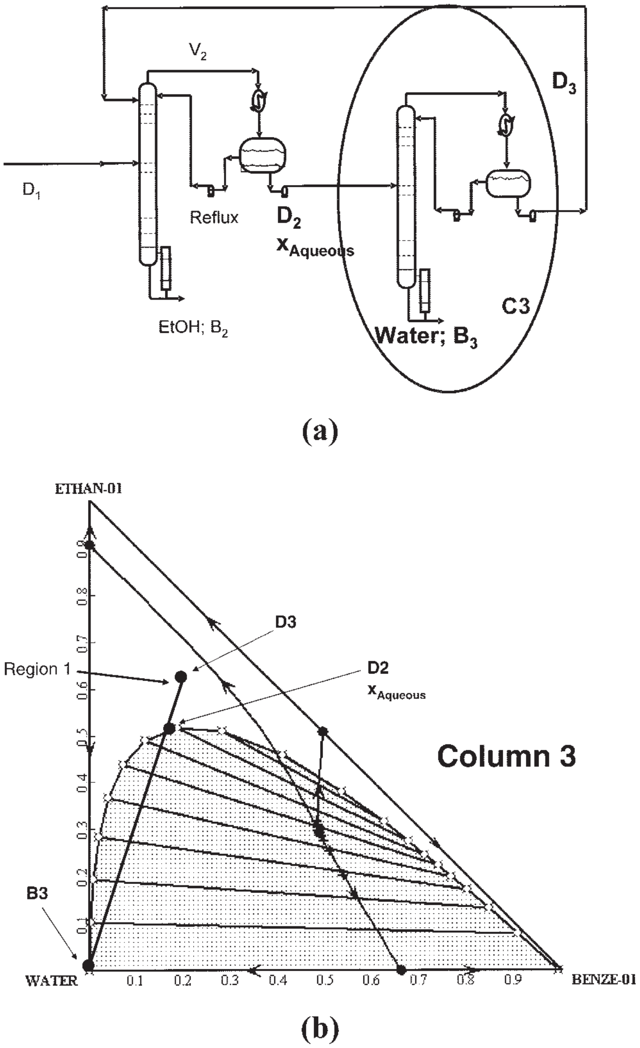

Figure 4. (A) Column C3; (B) location of streams in column C3.

state flowsheet. The first "preconcentrator" column is easily simulated. The same is not true of the last two columns because of the two recycle streams. Converging recycle streams is quite often very difficult. This is particularly true in this highly nonideal phase equilibrium system. The "strongly nonideal liquid" option is used in the distillation block for both columns C2 and C3. As shown by Chien and coworkers,[5] multiple steady states are possible in this type of system.

The azeotropic column C2 is very touchy. For example, if a large amount of organic reflux (100 kmol h^{-1}) is fed to the column, the bottoms B_2 contains very little water but too much benzene. As the organic reflux is slowly reduced, the amount of benzene in the bottoms grows increasingly smaller. The final design flow rate of organic reflux is 74 kmol^{-1} h^{-1}, which gives a benzene concentration of 0.5 mol % in the ethanol product and 0.4 mol % water.

However, if the simulation is initially run with an organic reflux of 74 kmol h^{-1}, the program will converge to a completely different steady state, which has about 18 mol % *water* in the bottoms.

Figure 8a gives the Aspen Plus flowsheet for columns C2 and C3. The recycle streams "REFLUX" and "RECYCLE" are not connected. Guesses were made of these two "tear" streams, and calculated values were obtained ("CALCREFL" and "CALCRECY'). The guessed values were manually adjusted until the guessed and the calculated values of flow rates, compositions, and temperatures were quite close (1–3% difference). Then the tear streams were connected and identified as such in the *Convergence* section of Aspen Plus. The flowsheet did *not* converge. Convergence could not be obtained using any of the available methods in the simulator. The flow rates of the recycle stream either went to zero or grew to very large values.

After many fruitless attempts, an alternative procedure to determine the steady-state solution was used. The flowsheet with the tear streams *not connected* was "exported" into AspenDynamics. Then the tear streams were connected in AspenDynamics by deleting either a "calculated " or "guessed " stream and reconnecting its "destination " or "source. " The

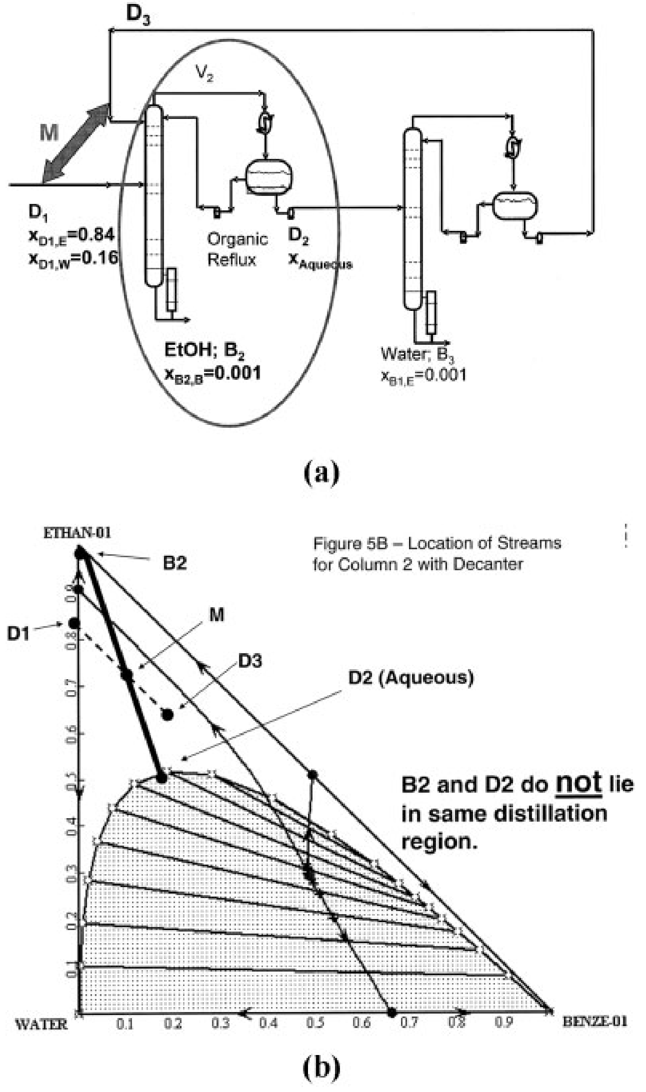

Figure 5. (A) Column C2 including the decanter; (B) location of streams for column C2 with decanter.

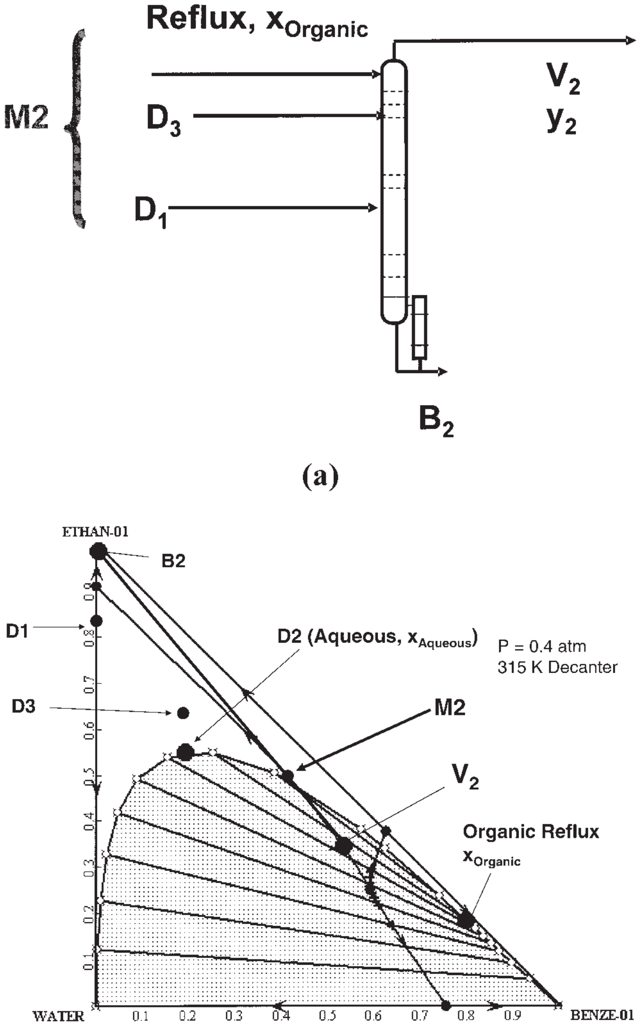

(a)

(b)

Figure 6. (A) Column C2 without the decanter; (B) location of streams for column C2 without decanter.

final flowsheet is shown in Figure 8b. Rigorous global properties were specified in AspenDynamics.

As additional evidence of the recycle convergence problems in a steady-state simulation, the precise converged values for "RECYCLE " and "REFLUX " obtained in the dynamic simulation were used in the Aspen Plus simulation as initial guesses. When the tear streams were closed, *convergence still failed.*

A plantwide control structure was developed during the course of converging the dynamic flowsheet. This is discussed in detail in the following section.

Dynamics and Control

The sizing of equipment is necessary to convert a steady-state simulation to a dynamic one. The *Tray Sizing* section of the distillation column block in Aspen Plus was used to determine column diameters.

Reflux drums and column bases were sized to provide 10 min of holdup when full. A holdup time of 20 min was used in the decanter. Pumps and valves were inserted to provide adequate pressure drops over valves for good rangeability. Most valves were specified to have pressure drops of 2 atm. The Aspen Plus file was pressure checked and export into Aspen-

Table 1. Design Values: Azeotropic Column C2

Pressure (atm)	2		
Temperature (K)			
Top	359		
Base	373		
Total stages	31		
Feed stages			
Reflux (organic)	1		
Recycle D_3	10		
Feed D_1	15		
Flow rates (kmol h^{-1})			
Reflux (organic)	74.0		
Recycle	53.9		
Feed	60.0		
Overhead vapor	137.1		
Bottoms	50.9		
Composition (mf)	Benzene	Ethanol	Water
Reflux	0.805	0.176	0.019
Recycle	0.215	0.642	0.143
Feed	0	0.840	0.160
Overhead vapor	0.518	0.347	0.135
Bottoms	0.005	0.991	0.004
Tray 28 liquid	0.07		
Reboiler heat (MW)	1.52		
Column diameter (m)	0.86		
Diameter/length (m)			
Base	1.1/2.2		

Table 2. Design Values: Entrainer Recovery Column C3 and Decanter

Entrainer Recovery Column C3			
Pressure (atm)	1.1		
Temperature (K)			
Reflux drum	342		
Base	373		
Total stages	21		
Feed stage	11		
Flow rates (kmol h^{-1})			
Distillate	53.9		
Feed (aqueous)	63.2		
Bottoms	9.4		
Composition (mf)	Benzene	Ethanol	Water
Distillate	0.215	0.642	0.143
Feed (aqueous)	0.183	0.546	0.271
Bottoms	0	0.001	0.999
Reboiler heat (MW)	1.8		
Reflux ratio	2		
Column diameter (m)	0.94		
Diameter/length (m)			
Reflux drum	1/2		
Base	0.7/1.4		
Decanter			
Temperature (K)	315		
Flow rates (kmol h^{-1})			
Organic	74		
Aqueous	63.2		
Compositions (mf)	Benzene	Ethanol	Water
Organic	0.805	0.176	0.019
Aqueous	0.183	0.546	0.271
Diameter (m)	2		
Length (m)	4		
Condenser heat removal (MW)		1.52	

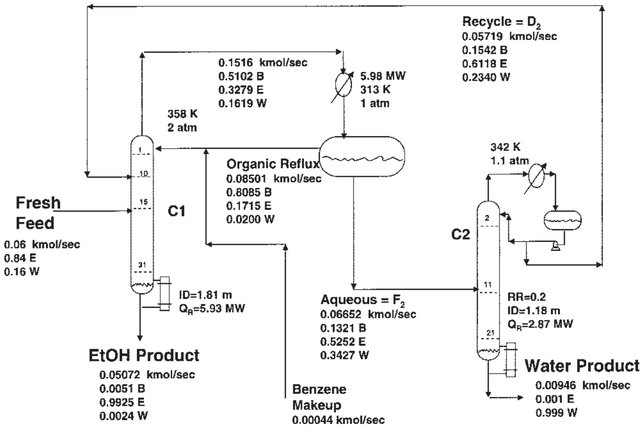

Figure 7. Steady-state conditions.

Dynamics. The default control scheme was modified as discussed in the following section.

Plantwide control structure

The critical element in a successful plantwide dynamic simulation is an effective and robust basic regulatory control scheme. Heuristic methods suggested by Luyben et al.[9] were used to develop the control structure shown in Figure 8. The various control loops are as follows:

(1) The fresh feed to column C2 is flow control. In the complete three-column system, the set point of the flow controller would be set by a level controller on the reflux drum of column C1.

(2) The flow rate of the organic reflux is ratioed to the fresh feed with the ratio being set by the composition controller CC2, to be discussed in Item (6) below.

(3) The heat input to the reboiler of column C2 is also ratioed to the fresh feed.

(4) The pressure in C2 is controlled by valve V13 in the vapor line.

(5) The base level in C2 is controlled by manipulating bottoms flow rate.

(6) The composition of benzene on Stage 28 of column C2 is controlled by adjusting the reflux-to-feed ratio, as discussed in Item (2). In a later section, a tray temperature will be used instead of composition.

(7) The temperature of the decanter feed is controlled by manipulating heat removal in the condenser HX2.

(8) The organic level in the decanter is controlled by manipulating the benzene makeup.

(9) The aqueous level in the decanter is controlled by changing the set point of the flow controller on the aqueous stream

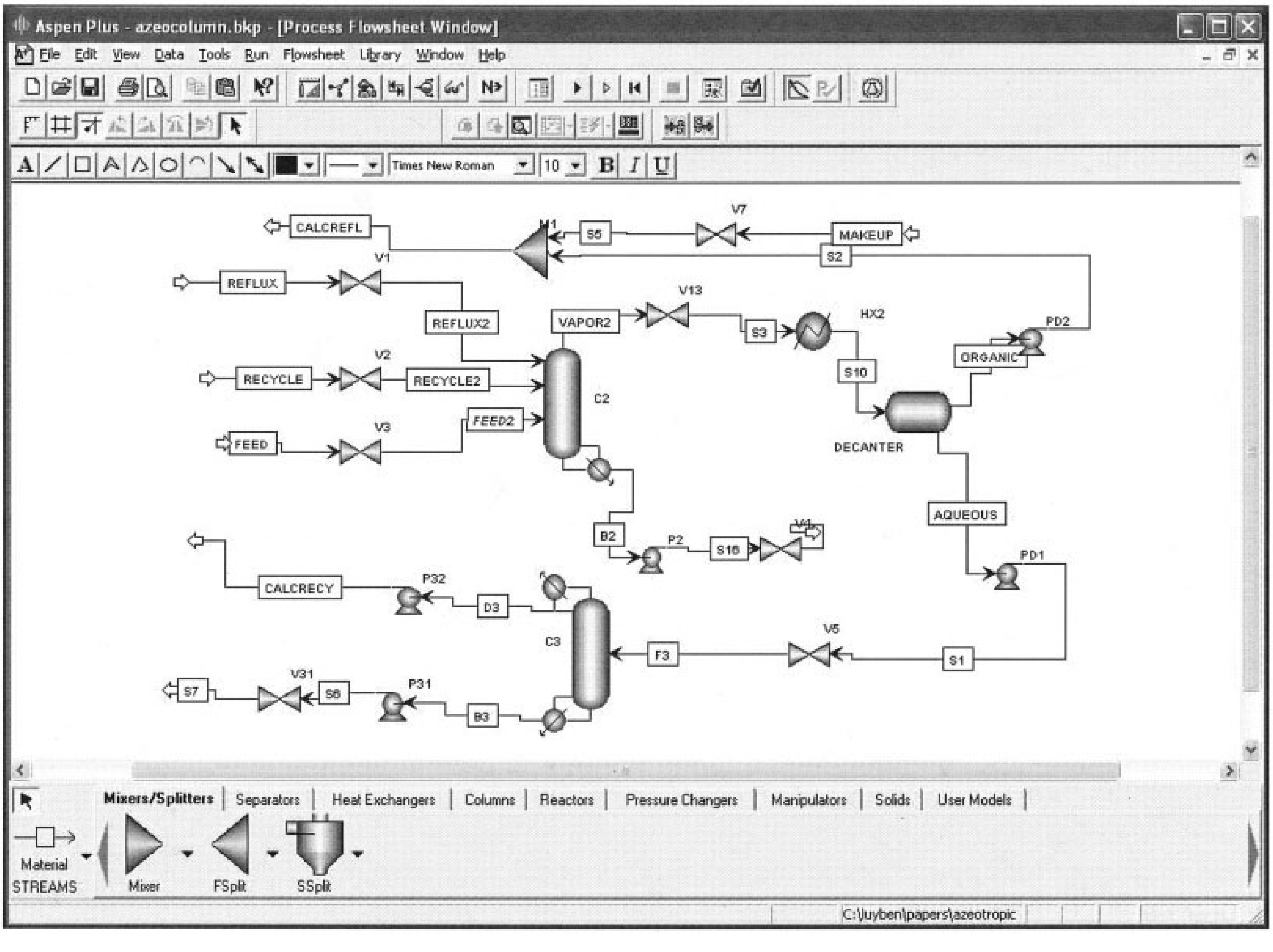

Figure 8a. Aspen Plus flowsheet with recycles not closed.

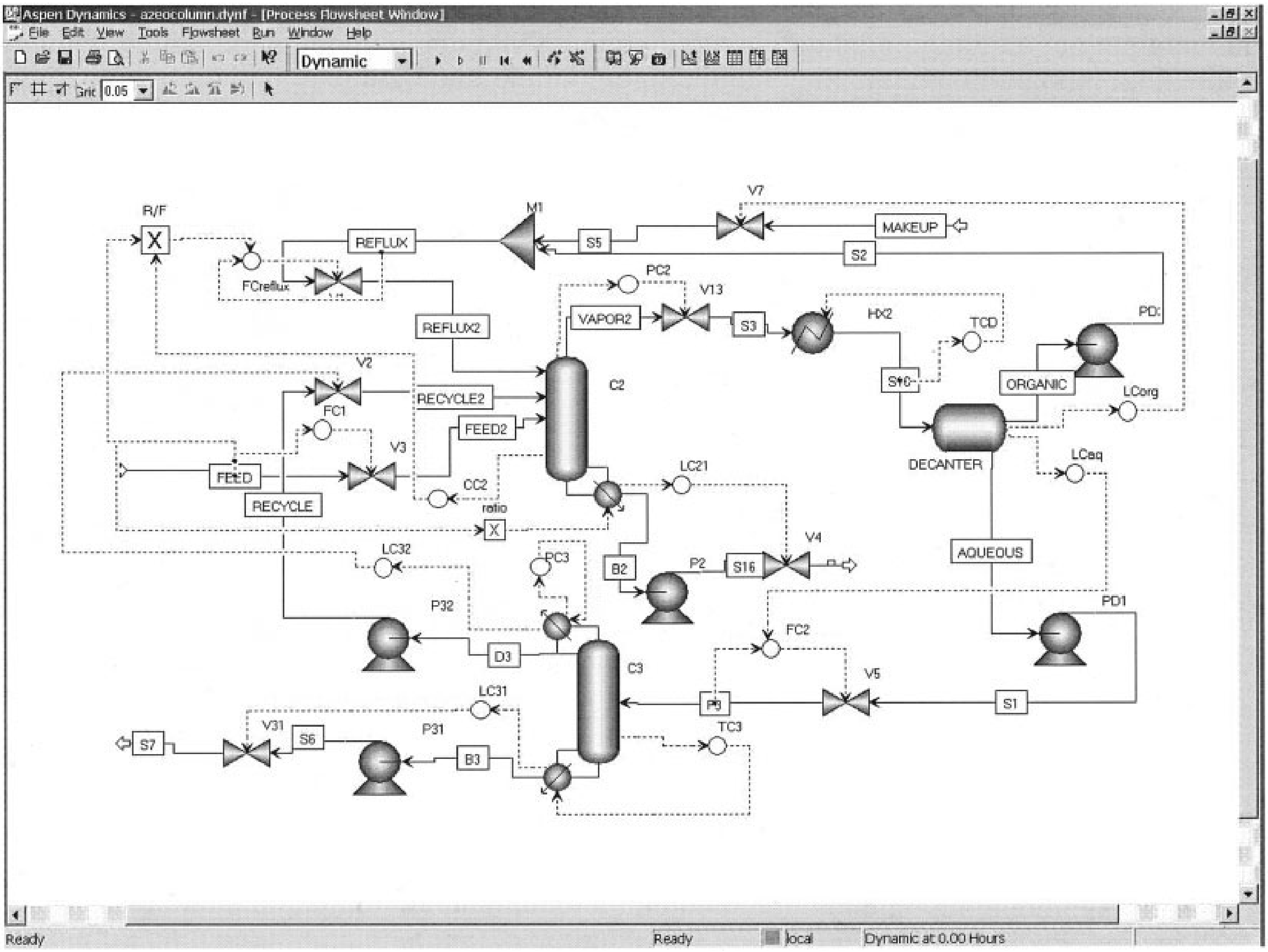

Figure 8b. AspenDynamics flowsheet with recycles connected.

(D_2 or F_3) that is fed to column C3. More will be said later about the very unusual action of the aqueous level controller. Certainly one would expect the level controller to be "direct acting " (an increase in level increases the aqueous flow).

(10) Pressure in column C3 is controlled by condenser heat removal.

(11) Reflux drum level in C3 is controlled by manipulating distillate flow D_3 (recycle fed to column C2).

(12) Base level in C3 is controlled by manipulating bottoms flow.

(13) The temperature on Stage 19 in column C3 is controlled by manipulating reboiler heat input.

(14) The mass flow rate of reflux in C3 is fixed.

Most of the loops discussed above are standard distillation control strategies. All flow controllers are PI with the normal settings: $K_C = 0.5$ and $\tau_I = 0.3$ min. All level loops are P-only with $K_C = 2$. The pressure controllers are PI and use Aspen-Dynamic default values. The tray pressure profiles are dynamically calculated in the simulator.

A 1-min dead time was inserted in the composition control loop in C2, and a relay-feedback test was run to achieve the ultimate gain and period. Then the Tyreus–Luyben setting were used: $K_C = 0.094$ and $\tau_I = 32$ min (with a composition transmitter range of 0 to 14 mol % benzene and controller output range of 0 to 2 feeding the reflux-to-feed ratio).

The interesting loops are Items (6), (9), and (13).

Temperature Control in C3. A temperature in column C3 can be used to inferentially control the purity of the water product leaving in the bottoms stream B_3. As shown in Figure 9A, there is a sharp temperature break at about Stage 19, which implies that temperature control should be effective.

Composition Control in C2. As Figure 9A also shows, the temperature profile in column C2 is quite flat. The only break is very near the bottom of the column, but even here temperature changes only about 1.5 K per tray. Therefore the use of temperature to maintain bottoms ethanol purity may not be effective. Small changes in pressure or the existence of other nonkey components could affect temperatures. So in the initial part of the study, a composition controller is used in column C2 to maintain bottoms ethanol purity. In a later section, the use of temperature will be explored and shown, somewhat surprisingly, to be fairly effective.

The intuitive place to measure purity is at the bottom of the column. However, this does not provide effective control because the purity level is quite high (0.5 mol % benzene) and changes very rapidly. By the time a disturbance is detected at the bottom of the column, the benzene profile has been driven away from the desired shape, and the column can easily "go over the cliff" to a situation where water comes out the bottom of the column.

Therefore, the composition on an intermediate tray is selected for composition control. Figure 9B gives composition profiles in C2. There is a sharp rise in benzene concentration from Stage 29 up to Stage 25. The benzene composition on Stage 28 is selected for control.

Level Control of Aqueous Phase in Decanter. The most unusual loop in this process is this level controller. Certainly one would expect that as the aqueous phase level increases, the aqueous flow from the decanter should be increased. This is the standard "direct acting" level controller manipulating an outflow stream from a unit. However, it was discovered that this level controller should be "reverse acting" to control level. This is certainly counter-intuitive.

The explanation for this can be seen in the results given in Figure 10. In Figure 10A, the aqueous level controller is put on manual with the aqueous flow controller on "automatic" with local set point, not "cascade." A step increase is made in the flow controller set point at time equal 0.1 h. The aqueous flow increases from 61 to 70 kmol h^{-1}. The aqueous level does *not* start to decrease as one would expect; instead it starts to increase after about 0.1 h. What is causing the unusual response?

The answer lies in the effect of the increase in aqueous flow on the recycle flow (the distillate D_3 from C3) going back to C2. This flow increases because the temperature controller in C3 sees a decrease in Stage 19 temperature. This puts more water into C2, which increases the concentration of water y_{2W} in the vapor leaving the top of C2 and entering the decanter. The result is a shift in the organic and aqueous split entering the decanter, which produces more aqueous phase. As shown in Figure 10A, the organic level decreases and the aqueous level increases.

A second test is shown in Figure 10B in which several controllers are put in manual in addition to the aqueous level controller. The temperature controller in C3 and the composition controller in C2 are both put on manual. This means that the heat inputs to the two columns are fixed. The aqueous level remains almost constant, despite the increase in the aqueous flow from the decanter. The recycle flow rate D_3 still increases slightly even with a fixed reboiler heat input, which probably arises from composition changes and latent heat of vaporization differences. The increase in the composition of the water in the vapor from C2 ("y2W" in Figure 10B) is slower, but it still increases. The drop in the organic level is larger because the reflux flow rate is fixed.

Control effectiveness

The effectiveness of the plantwide control structure was tested by making large disturbances in the feed composition and feed flow rate. Results are given in Figure 11. The responses to disturbances in both feed composition (solid lines) and feed flow rate (dashed lines) are shown.

The feed composition is changed from 84/16 mol % ethanol/water to 80/20 mol % at time = 0.2 h. This is a 25% increase in the water in the feed. Then at 7.5 h, the feed composition is changed to 88/12 mol % ethanol/water, a 40% decrease in the water fed to the system. These are quite large step changes for a "touchy" azeotropic distillation process to handle. The control structure handles these large feed composition disturbances very well. Product purities x_{B2} and x_{B3} remain very close to the desired levels.

The disturbances in the flow rate of the feed are step changes. At time = 0.2 h, the set point of the feed flow controller is increased from 60 to 72 kmol h^{-1}, a 20% step disturbance. At time = 7.5 h, the set point is dropped to 48 $kmol^{-1}$ h^{-1}, an extraordinary 40% reduction. Figure 11 shows how the system response to these very large feed flow rate disturbances. When feed increases, reflux, recycle, aqueous phase flow F_3, and ethanol product B_2 all increase. The two ratios produce immediate changes in reflux and heat input. The composition controller in column C2 adjusts the reflux-to-feed ratio to bring the benzene concentration on Stage 28 back to 7 mol %.

The purity of the water product x_{B3} is maintained very near its steady-state value by the Stage 19 temperature controller in C3. The purity of the ethanol product x_{2B} undergoes some short-term departures from its desire level, particularly when feed flow rate is decreased, but it returns to the desired 99 mol % purity.

Figure 12 shows the faceplates of all controllers. Note that the FC2 controller is on "cascade" because it receives its set point signal from the decanter aqueous level controller. Likewise the FC reflux controller is on cascade because its set point signal comes from the reflux-to-feed ratio element.

Higher-Purity Design

Chien[10] suggested, in a very thorough and knowledgeable review of this paper, that the counter-intuitive aqueous level control loop may be a function of the purities of the products. To explore this possibility, an additional process design was developed in which the ethanol purity was increased from 99 to 99.9%. Additional trays were added to the column (61 stages). The organic reflux was increased from 74 to 87 kmol h^{-1}, and the recycle D_3 was increased from 53.9 to 66 kmol h^{-1}. This increased the reboiler heat input in C2 and C3 from 1.50 and 1.80 to 1.78 and 2.19 MW, respectively.

Figure 13A compares the temperature profiles of the moderate and high purity designs, which are quite similar. Note that the temperatures in the lower section of the high-purity case are higher because of the additional pressure drop resulting from having more trays.

Figure 13B gives the composition profiles in C2 for the high-purity case. These should be compared with those given in Figure 9B for the moderate-purity case. The shapes are quite similar.

The control structure with the counter-intuitive aqueous level controller was tested, with results showing that it also works in the high-purity case. Thus the unusual behavior is not a result of purity levels.

Temperature Control in C2

Chien[10] also suggested temperature control in C2 should be explored instead of composition control, despite the small temperature changes. The moderate-purity design was stud-

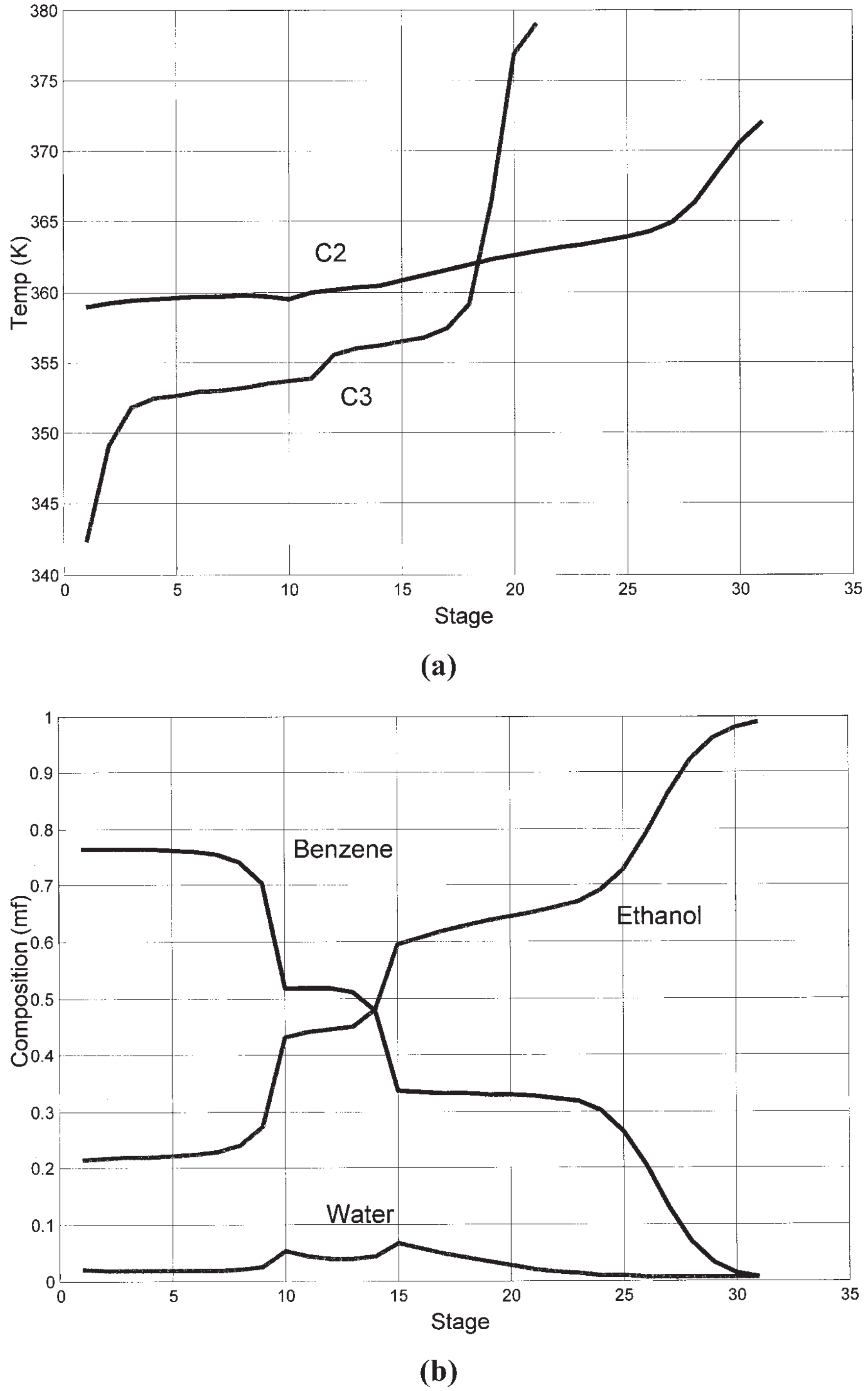

(a)

(b)

Figure 9. (A) Temperature profiles in C2 and C3; (B) composition profiles in C2.

ied in which the temperature change from the base to the lower plateau in the stripping section of the column is only about 8 K. The temperature on Stage 28 was selected and was controlled by manipulating organic reflux (actually the reflux-to-feed ratio).

A 1-min dead time was inserted in the temperature control loop in C2, and a relay-feedback test was run to achieve the ultimate gain and period. Then the Tyreus–Luyben settings were used: $K_C = 2.6$ and $\tau_I = 33$ min (with a temperature transmitter range of 300 to 400 K and controller output range of 0 to 2 feeding the reflux-to-feed ratio).

Figure 14 gives dynamic simulation results using this temperature control strategy for feed composition and feed flow rate disturbances. Somewhat unexpectedly, at least to the author, the structure worked quite well.

However, Figure 15 shows what happens if changes in pressure occur when using the temperature control structure. A series of step changes in the set point of the C2 pressure control

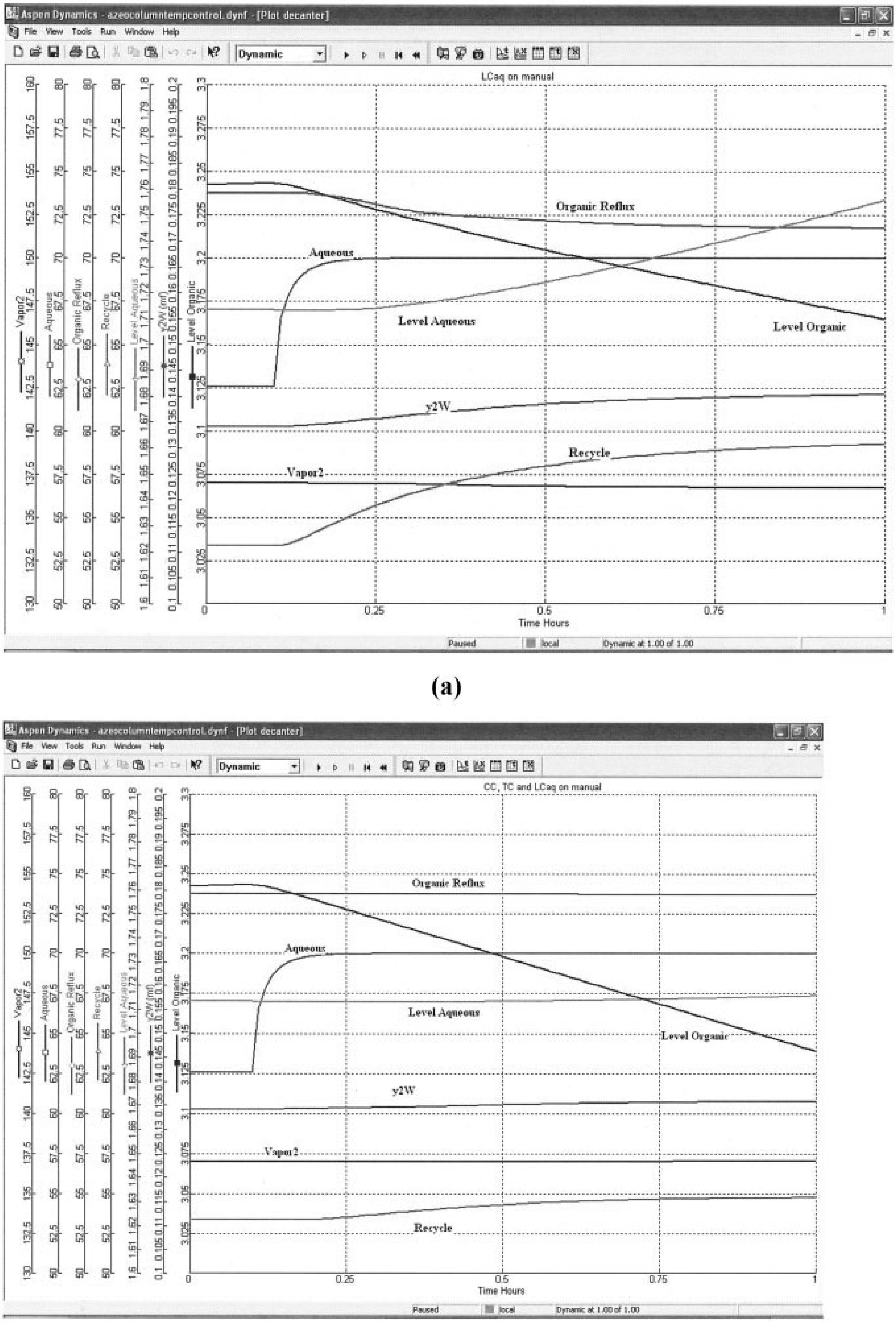

(a)

(b)

Figure 10. (A) Decanter responses with only aqueous LC on manual; (B) decanter responses with several loops on manual.

are made starting at 2 atm and ending at 2.3 atm. As the pressure increases, with a constant control tray temperature, the purity of the bottoms ethanol product drops. These results illustrate the sensitivity of a plain temperature control scheme. The use of pressure-compensated temperature should alleviate this potential problem.

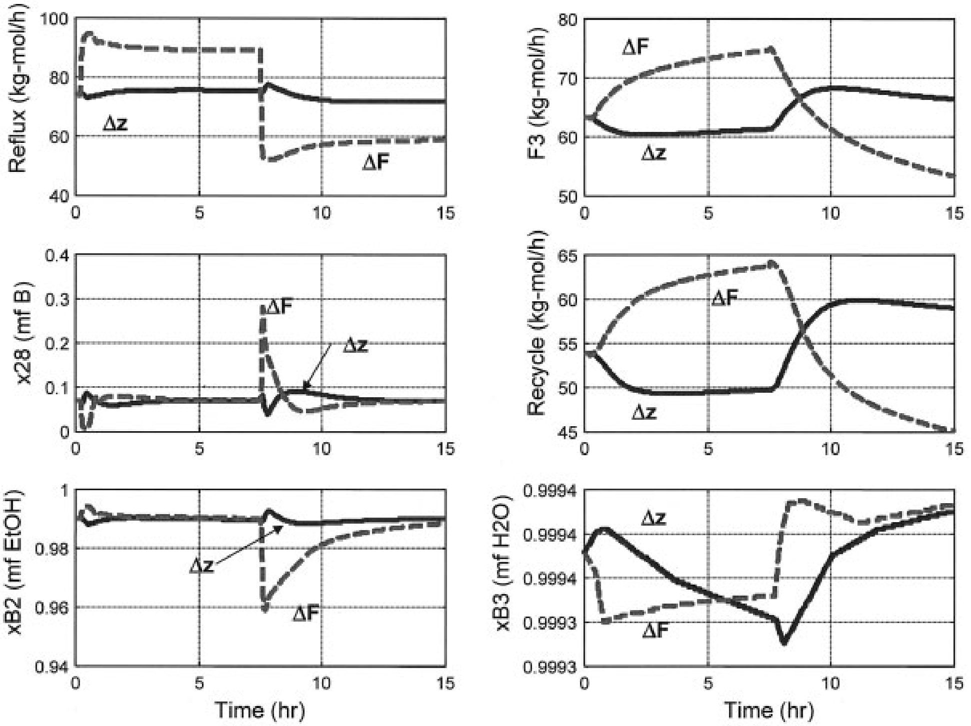

Figure 11. Responses to feed composition and feed flow changes.

Conclusion

This article presents a study of the control of a two-column heterogeneous azeotropic system separating ethanol and water using benzene as the light entrainer. The difficulty of converging the steady-state flowsheet because of the two recycle streams is discussed. This problem is solved by converting to a dynamic simulation.

A plantwide control structure is developed and tested, providing effective base-level regulatory control of this highly nonideal and interacting system.

An unusual level control strategy is used to control the level of the aqueous phase in the decanter. The action of the controller is the reverse of what conventional wisdom dictates. This occurs because of the effect of changing the aqueous flow on conditions in all of the units: azeotropic column, decanter, and entrainer recovery column.

One of the reviewers of this article stated that the counter-intuitive level controller action is “fairly standard for this separation configuration ” and “is well known, at least to practitioners. ” The reviewer also stated that “the explanation presented in this contribution is completely consistent with what I have understood previously,” which was that “if the bottoms is controlled tightly (whether or not to high purity) and the top is allowed to vary as a function of reflux and recycle

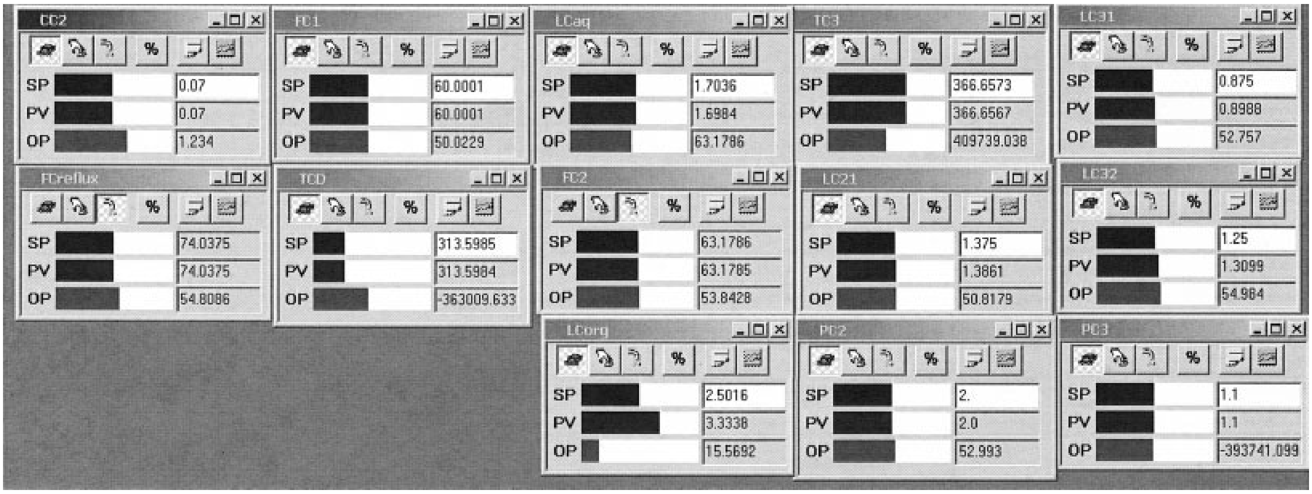

CC2
SP 0.07
PV 0.07
OP 1.234

FC1
SP 60.0001
PV 60.0001
OP 50.0229

LCaq
SP 1.7036
PV 1.6984
OP 63.1786

TC3
SP 366.6573
PV 366.6567
OP 409739.038

LC31
SP 0.875
PV 0.8988
OP 52.757

FCreflux
SP 74.0375
PV 74.0375
OP 54.8086

TCD
SP 313.5985
PV 313.5984
OP -363009.633

FC2
SP 63.1786
PV 63.1785
OP 53.8428

LC21
SP 1.375
PV 1.3861
OP 50.8179

LC32
SP 1.25
PV 1.3099
OP 54.984

LCorg
SP 2.5016
PV 3.3338
OP 15.5692

PC2
SP 2.
PV 2.0
OP 52.993

PC3
SP 1.1
PV 1.1
OP -393741.099

Figure 12. Controller faceplates.

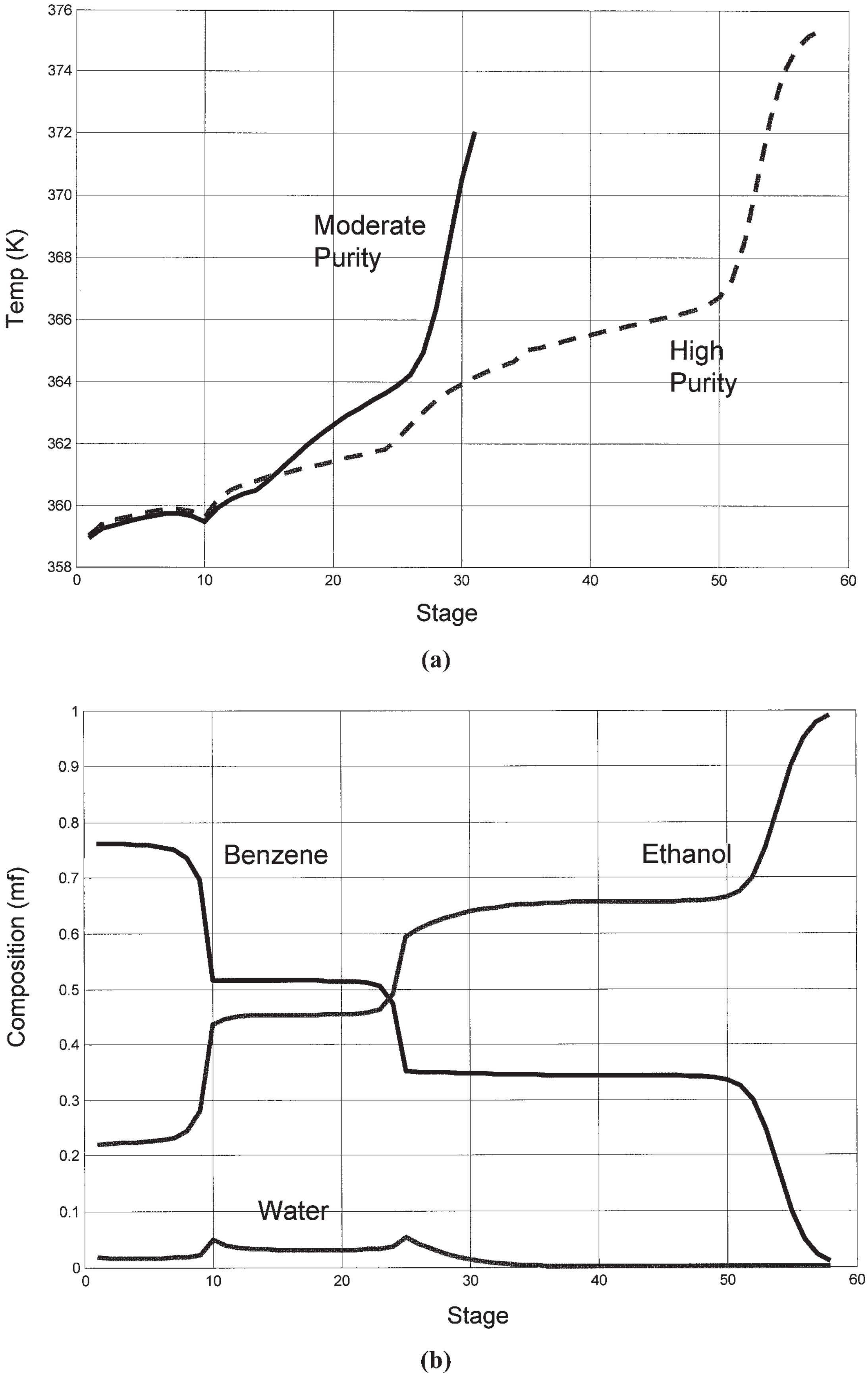

Figure 13. (A) Temperature profiles in C2 with high and moderate purities; (B) composition profiles in C2 with high purity.

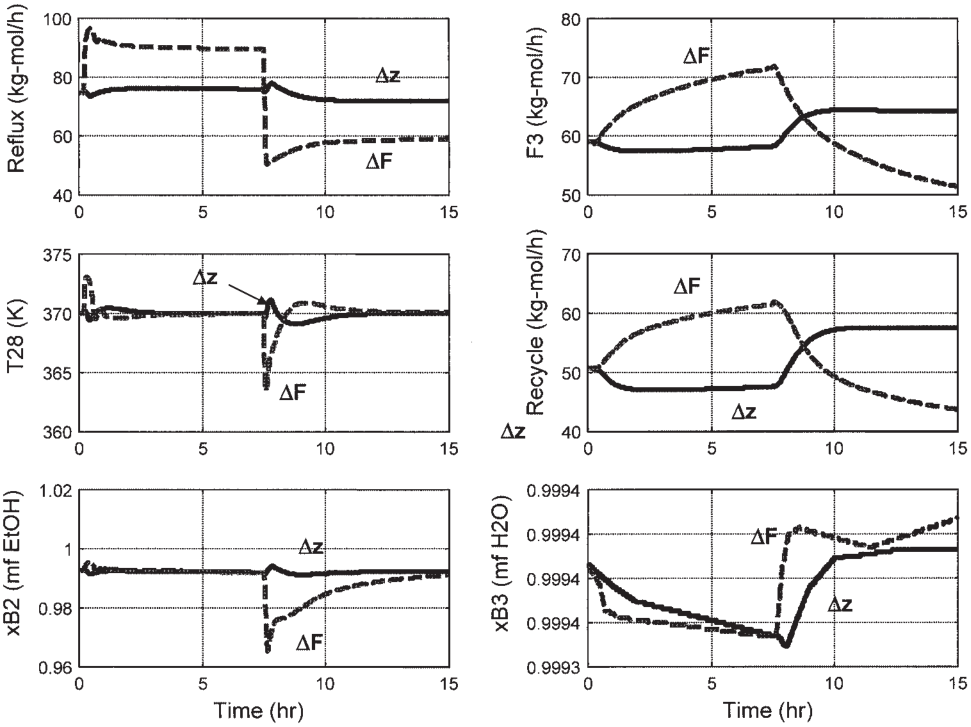

Figure 14. Responses with temperature control in C2.

flows/compositions, then the observed behavior occurs and the normal practice is for a reverse-acting aqueous level controller." This provides important validation of the results presented in this article and indicates that the counter-intuitive control structure is not just the result of a bug in the simulation software.

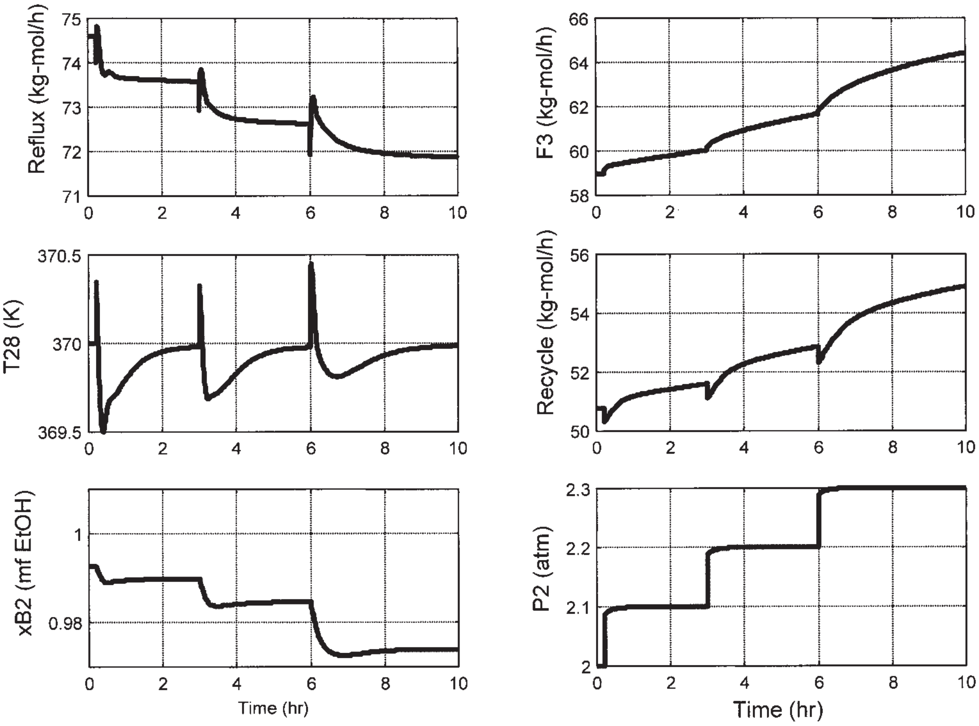

Figure 15. Response for pressure changes with temperature control in C2.

Notation

B_n = bottoms product from column n, kmol h^{-1}
Cn = column n
D_n = distillate product from column n, kmol h^{-1}
F = feed flow rate to column C1, kmol h^{-1}
F_3 = feed flow rate to column C3, sometimes called D_2, kmol h^{-1}
K_C = controller gain, dimensionless
V_2 = vapor from column C2, kmol h^{-1}
x_{Aqueous} = composition of aqueous phase, mole fraction
x_{B2} = composition of ethanol product, mole fraction ethanol
x_{B3} = composition of water product, mole fraction water
x_{Organic} = composition of organic phase, mole fraction
y_2 = composition of V_2, mole fraction
τ_{I} = controller integral time, min

Literature Cited

1. Robinson CS, Gilliland ER. *Elements of Fractional Distillation*. 4th Edition. New York, NY: McGraw-Hill; 1950:312 [First published in 1922.]
2. Doherty MF, Malone MF. *Conceptual Design of Distillation Systems*. New York, NY: McGraw-Hill; 2002:371.
3. Stichlmair JG, Fair JR. *Distillation: Principles and Practices*. New York, NY: Wiley–VCH; 1998:238.
4. Ryan PJ, Doherty MF. Design/optimization of ternary heterogeneous azeotropic distillation systems. *AIChE J.* 1989;35:1592.
5. Chien IL, Wang CJ, Wong DSH. Dynamics and control of heterogeneous azeotropic distillation column: Conventional control approach. *Ind Eng Chem Res.* 1999;38:468.
6. Chien IL, Wang CJ, Wong DSH, Lee CH, Cheng SH, Shih RF, Liu WT, Tsai CS. Experimental investigation of conventional control strategies for a heterogeneous azeotropic distillation column. *J Process Contr.* 2000;10:333.
7. Chien IL, Chen WH, Chang TS. Operation and decoupling control of a heterogeneous azeotropic distillation column. *Comput Chem Eng.* 2000;24:893.
8. Chien IL, Choa HY, Teng YP. Design and control of a complete heterogeneous azeotropic distillation column system. *Proc PSE Asia.* 2002:213-218.
9. Luyben WL, Tyreus BD, Luyben ML. *Plantwide Process Control*. New York, NY: McGraw-Hill; 1999.
10. Chien IL. National Taiwan University of Science and Technology. Private communication; 2004.

Manuscript received Jan. 18, 2005, and revision received Jun. 27, 2005.